J. Mater. Environ. Sci. 5 (2) (2014) 553-564
ISSN: 2028-2508
CODEN: JMESCN

Enhanced corrosion resistance properties of mild steel in neutral aqueous solution by new ternary inhibitor system

M. Prabakaran, K. Vadivu, S. Ramesh*, V. Periasamy
Department of Chemistry, The Gandhigram Rural Institute, Deemed University, Gandhigram-624302, Dindigul, Tamilnadu, India

Received 24 Sept 2013, Revised 2 Dec 2013, Accepted 2 Dec 2013
** Corresponding author. E mail: drsramesh_56@yahoo.com ; Tel: +91(0)451-2452371.*

Abstract
The goal of studying corrosion process is to find means of minimizing corrosion or prevent it from occurring. The use of inhibitors is one of the most popular methods for corrosion protection. A protective film has been formed on the surface of mild steel in neutral aqueous environment using a synergistic mixture of an eco-friendly inhibitor viz., Vitamin B1 (Thiamine hydrochloride) along with Iminodi(methylphosphonic acid) (IDMPA) and Zn^{2+} ions. The inhibitive effect of Vitamin B1, IDMPA and Zn^{2+} ions has been investigated by gravimetric studies, potentiodynamic polarization and electrochemical impedance spectroscopy (EIS). The investigations revealed that Thiamine acts as an excellent synergist in corrosion inhibition. Optimum concentrations of all the three components of the ternary formulation are established by gravimetric studies. Potentiodynamic polarization studies inferred that this mixture functions as a mixed inhibitor. EIS studies of the metal/solution interface indicated that the surface film is highly protective against the corrosion of mild steel. Surface characterization techniques (FTIR, SEM and AFM) are also used to ascertain the nature of the protective film. The mechanistic aspect of corrosion inhibition is proposed.

Keywords: Corrosion, Mild steel, Gravimetric, Thiamine, Polarization, Protective film.

Introduction
Inhibition of corrosion of mild steel is a matter of theoretical as well as practical importance [1]. The use of inhibitors is one of the most economical and practical methods of reducing corrosive attack on metals [2, 3]. The use of organic molecules as corrosion inhibitor is one of the most practical methods for protecting against the corrosion and it is becoming increasingly popular [4]. The molecules most often used as corrosion inhibitors are nitrogen, sulphur, oxygen and phosphorus containing compounds [5-7]. These compounds get adsorbed onto the surface of metal from the bulk of environment forming a protective film at the metal surface [8]. The inhibition efficiency increases in the order O<N<S<P [9].

The application of phosphonic acid inhibitors is a widely used, inexpensive way to protect the metals from corrosion. Phosphonic acid derivatives alone or together with other additives can effectively inhibit the corrosion of metals [10-12]. Phosphonic acids have been widely used as water treatment agents because of their low toxicity, high stability and corrosion inhibition activity in neutral aqueous media [13]. Compounds with a phosphonic functional group are considered to be the most effective chemicals for inhibiting the corrosion process and it is well known that short-chain-substituted phosphonic acids are good corrosion inhibitors for iron and low alloyed steels [14]. Phosphonate based formulations are well known as corrosion inhibitors in aqueous environments [15-17]. Synergistic effect existing between phosphonic acid and zinc ions on the inhibition of metals corrosion has already been studied by several researchers [18-20]. In this background, a new ternary inhibitor formulation with relatively low concentration of both phosphonate and Zn^{2+} in the presence of an organic compound has been proposed in the present study. The selected phosphonic acid and the organic compound are iminodi(methylphosphonic acid) (IDMPA) and Vitamin B1 (Thiamine hydrochloride), respectively. IDMPA consists of two phosphonic acid groups. In the present study was carried out using an environmentally friendly organic compound namely Thiamine as a synergist to the binary formulation containing IDMPA and zinc ions for corrosion control of mild steel. The formulations are refered to as ternary inhibitor systems. A few of such formulations were reported in the literature [15-17, 21]. Thiamine is chosen as the synergist for the present study due to presence of one amino group and one hydroxyl group in its structure,

which provide complexing ability with metal ions. The main objective of the present study is to investigate the inhibitory effects of the new ternary inhibitor formulation containing IDMPA, Zn^{2+} and Thiamine in corrosion inhibition of mild steel in an aqueous environment containing 60 ppm chloride using gravimetric method and electro chemical methods. Also, it is of interest to study the synergistic effect of Thiamine in combination with IDMPA and Zn^{2+} on corrosion inhibition. Surface analytical techniques were also used to investigate the nature of the surface film and a suitable mechanism of corrosion inhibition is proposed. For all these studies, aqueous solution of 60 ppm chloride has been chosen as control because of the water used in cooling water systems is generally either demineralized water or unpolluted surface water.

2. Materials and methods

2.1. Materials

IDMPA ($C_2H_9O_6P_2N$), zinc sulphate ($ZnSO_4.7H2O$), Thiamine ($C_{12}H_{17}N_4OSCl$) and other reagents were analytical grade chemicals. The molecular structures of IDMPA and thiamine are shown in **Figs. 1** and **2** respectively. All the solutions were prepared by using triple distilled water. pH values of the solutions were adjusted by using 0.01 N sodium hydroxide and 0.01 N sulphuric acid solutions. An aqueous solution consisting of 60 ppm of sodium chloride has been used as the control through out the studies.

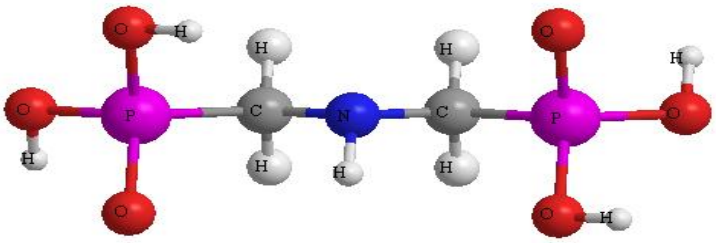

Figure 1: The molecular Structure of IDMPA

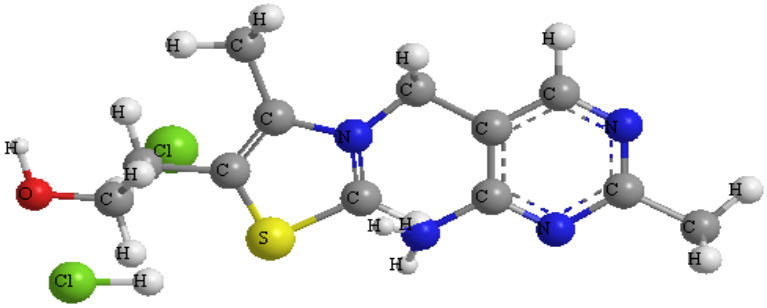

Figure 2: The molecular structure of Thiamine

2.2. Preparation of specimens

For all the studies, the specimens taken from a single sheet of mild steel of the following composition were chosen: C, 0.1–0.2%; P, 0.03–0.08%; S, 0.02–0.03%; Mn, 0.4–0.5% and the rest iron. For gravimetric measurements and surface analytical techniques, the polished specimens of the dimensions, 3.5 cm x 1.5 cm x 0.2 cm, were used while for other (electro chemical) studies, the dimensions of the specimens were 1.0 cm x 1.0 cm x 0.1 cm. Prior to all measurements, the specimens were polished successively using 1/0 to 6/0 emery papers, degreased with trichloroethylene and washed thoroughly with triple-distilled water and dried.

2.3. Gravimetric studies

Gravimetric experiments are the easiest way to find the corrosion rate (CR) and inhibition efficiency (IE). In all gravimetric experiments, the polished specimens were weighed and immersed in duplicate, in 100 ml control solution in the absence and presence of inhibitor formulations of different concentrations, for a period of 7 days. Then, the specimens were reweighed after washing and drying. The weights of the specimens before and after immersion were determined with Mettler electronic balance AE 240 model with a readability of 0.1 mg. Accuracy in weighing up to 0.0001 g and its surface area measurement up to 0.1 cm^2, as recommended by ASTM, was followed. Corrosion rates of mild steel in the absence and presence of various inhibitor formulations are expressed in mdd. The corrosion rate was calculated according to the following equation

$$CR(mdd) = \left[\frac{\Delta W}{St}\right] \times 100 \quad (1)$$

where ΔW (mg) is the weight loss, S (cm^2) is the surface area and t (days) is the immersion period. Inhibition efficiencies (IE) of the inhibitor were calculated by using the formula

$$IE_g(\%) = \left[\frac{CR_0 - CR_I}{CR_0}\right] \times 100 \quad (2)$$

where CR_O is the corrosion rate in the absence of inhibitor and CR_I is the corrosion rate in the presence of inhibitor

2.4. Electrochemical studies

The CHI electrochemical analyzer Model 760D was used to record Tafel polarization curve and impedance curve. The mild steel specimens used as working electrode while platinum and calomel electrodes were used as counter electrode and the reference electrode, respectively. The working electrode was immersed in control solution for approximate 30 min until a steady-state open-circuit potential (OCP) was obtained. Impedance measurements were carried out at E_{corr} potential at the range of 100 kHz to 10 mHz at amplitude of 10 mV. The impedance diagrams are given in Nyquist representation. The impedance and polarization parameters such as double layer capacitance (C_{dl}), charge transfer resistance (R_{ct}), corrosion current (I_{corr}), corrosion potential (E_{corr}), anodic Tafel slope (β_a) and cathodic Tafel slope (β_C) were computed from the polarization curves and Nyquist plots.

The potentiodynamic polarization curves were recorded from -200 to +200 mV (versus OCP) with a scan rate of 1 mV s^{-1}. The IE_p values were calculated from potentiodynamic polarization measurements using the Eq. (3),

$$IE_P(\%) = \left[\frac{I_{corr} - I'_{corr}}{I_{corr}}\right] \times 100 \quad (3)$$

where I_{corr} and I'_{corr} are the corrosion current densities in case of the control and inhibitor solutions respectively.

To obtain the double layer capacitance (C_{dl}), the frequency at which the imaginary component of the impedance is maximum ($-Z_{max}$), is found and C_{dl} values are obtained from the equation

$$f(-Z_{max}'') = \frac{1}{2\pi C_{dl} R_{ct}} \quad (4)$$

From impedance measurements, the IE_I values were calculated from the following relation,

$$IE_I(\%) = \left[\frac{R'_{ct} - R_{ct}}{R'_{ct}}\right] \times 100 \quad (5)$$

where R_{ct} and R'_{ct} are the charge transfer resistance values in the absence and presence of the inhibitor respectively.

2.5. Surface analytical studies

The nature of the film formed on the surface of the metal specimen was analyzed by Fourier transform infrared spectroscopy (FTIR) and Scanning electron microscopy (SEM).

2.5.1. FTIR spectra

The mild steel specimens were immersed in various test solutions for a period of seven days. On completion of the 7^{th} day, the specimens were taken out and dried. The protective film formed on the metal specimens was scratched and mixed with KBr and pellets were obtained and the FTIR spectra were recorded using JASCO 460 PLUS Spectrophotometer over a range of 400-4000 cm^{-1} with a resolution of 4 cm^{-1}.

2.5.2. Scanning electron microscopy

The surface morphology of the formed layers on the mild steel surface after its immersion in control solutions containing 60 ppm chloride ions in the absence and in the presence of the inhibitor were carried out. After 7 days, the specimens were taken out, washed with distilled water and dried. The SEM photographs of the surfaces of the specimens were investigated using a VEGA3-TESCAN model scanning electron microscope.

2.5.3. Atomic force microscopy

Atomic force microscope was used for surface morphology studies. The protective films were examined with atomic force microscope (AFM) Nano Surf Easy Scan-2. The topography of the entire samples for a scanned area of 5 µm x 5µm (25µm2) is evaluated for a set point of 20 nN and a scan speed of 10 mm/s. The three and two dimensional topography of surface films gave various roughness parameters of the film.

3. Results and discussion

3.1. Gravimetric Studies

The inhibition of corrosion by phosphonic acids can be explained in terms of adsorption on the metal surface [11]. Phosphonic acids can be adsorbed on the mild steel surface by the interaction between lone pairs of electrons of nitrogen, oxygen, and phosphorus atoms of the inhibitor and the metal surface. This process is facilitated by the presence of vacant orbitals of low energy in iron atoms, as observed in the transition metals [22]. The gravimetric measurements were carried out to calculate the corrosion rate (CR) and inhibition efficiency (IE) for the mild steel in an aqueous solution containing 60 ppm chloride ions (control solution) in the absence and presence of various inhibitor formulations consists in various amounts of IDMPA, Zn^{2+} ions and Thiamine are given in **Table 1**. The inhibition efficiency was represented as a function of Thiamine ion concentration in **Fig. 3**.

Table 1: Corrosion rate (CR) and inhibition efficiency (IE) by gravimetric studies of mild steel in the presence of inhibitor

IDMPA (ppm)	Thiamine (ppm)	Zn^{2+} (ppm)					
		10		**20**		30	
		CR	IE	CR	IE	CR	IE
10	10	10.40	22	8.10	39	7.89	41
	25	9.80	26	7.36	45	8.77	34
	50	7.56	43	7.02	47	8.34	37
	75	7.83	41	6.18	54	9.87	26
	100	7.61	43	3.54	73	8.64	35
	150	9.43	29	4.92	63	8.55	36
	200	9.30	30	3.54	73	9.28	30
	250	7.03	47	3.09	77	8.53	36
20	10	8.68	35	10.61	20	5.54	58
	25	8.95	33	7.67	42	8.53	36
	50	6.97	48	5.97	55	7.67	42
	75	5.60	58	1.75	87	7.51	44
	100	4.41	67	1.31	90	4.65	65
	150	5.54	58	1.97	85	1.10	92
	200	6.87	48	1.43	89	1.39	90
	250	4.93	63	1.53	88	3.60	73
30	10	8.71	35	5.34	60	6.65	50
	25	8.84	34	4.88	63	5.65	58
	50	5.85	56	4.05	70	7.51	44
	75	6.89	48	1.97	85	3.51	73
	100	4.50	66	**0.72**	**95**	2.15	84
	150	6.69	50	0.72	95	0.75	94
	200	7.46	43	1.08	92	0.98	93
	250	6.03	55	1.18	91	1.48	89

The combination consists of 100 ppm IDMPA and 50 ppm Zn^{2+} ions wherein the maximum inhibition efficiency of 99% is obtained. An effort has been taken to reduce the concentrations of the synergistic components viz., IDMPA and Zn^{2+} ions. An environmentally friendly compound in the form of Thiamine hydrochloride (Vitamin B1) was chosen, added and the ternary system was studied. Further, the addition of Thiamine ions has not only increased the inhibition efficiency of mild steel, but also reduced environmental pollution because relatively lower concentrations of IDMPA and Zn^{2+} were sufficient to achieve good inhibition efficiency. Moreover, Thiamine is cheaper. Hence, it was decided to fix the concentration of both Zn^{2+} ions and IDMPA at levels below 30 ppm and vary the concentration of Thiamine in the range of 10 ppm to 250 ppm consisting of 72 different concentration systems. From the gravimetric studies, it is evident that for any protection to be established, a minimum concentration of each of the inhibitor constituent is necessary. It can be

seen from the results of the ternary formulations, that for lower concentration of 10 ppm Zn^{2+} and 20 ppm IDMPA with 100 ppm Thiamine, the maximum inhibition efficiency of only 67% is achieved. To achieve an inhibition efficiency of more than 90%, the required minimum concentration of IDMPA and Zn^{2+} are 30 ppm and 20 ppm respectively in presence of Thiamine. While the binary system consisting of 20 ppm Zn^{2+} and 30 ppm IDMPA gives only 33% inhibition efficiency. With the addition of Thiamine, the inhibition efficiency of the ternary formulation increased gradually with increase in concentration of Thiamine (95%) at 100 ppm. Further on increasing the concentration of Zn^{2+} from 20 ppm to 30 ppm, with 30 ppm IDMPA followed by increasing concentration of Thiamine, the same trend of inhibition efficiency is observed. It is worth mentioning that on addition of Thiamine, the concentration of IDMPA was reduced from 100 ppm to 30 ppm and the concentration of Zn^{2+} ions could be reduced from 50 ppm to 20 ppm to achieve good inhibition efficiency.In other words, the ternary systems were much more effective at very lower concentrations of IDMPA and Zn^{2+}. And this was the desired result. This formulation was chosen as the best inhibitor system for further studies. The combination of 20 ppm of Zn^{2+}, 30 ppm of IDMPA and 100 ppm of Thiamine was confirmed to be the best inhibitor system from the gravimetric data. A multi-coloured thin protective film was formed on the metal surface.

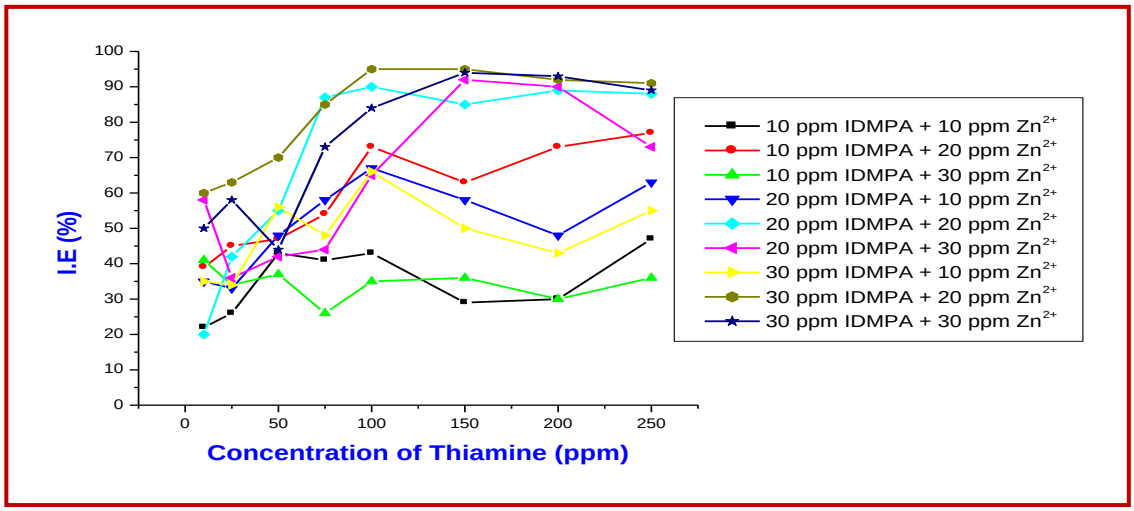

Figure 3: Inhibition efficiency as a function of concentration of Thiamine

3.1.2. Effect of pH

The influence of pH on corrosion rate of carbon steel in the presence of inhibitor system and the maximum inhibition efficiency obtained in the gravimetric measurements were studied. The effect of pH for the synergistic formulation consisting of IDMPA (30 ppm) + Zn^{2+} (20 ppm) + Thiamine (100 ppm) in the pH range of 3-11 is shown **Fig. 4**. The highest inhibition efficiency could be obtained in the pH range 5-8. But, when the pH is decreased from 5-3, the inhibition efficiency is reduced to 26 % and on increasing pH range from 8-11, the inhibition efficiency is reduced to 28 %. The reasons for decrease in inhibition efficiency in more alkaline and acidic environments are explained under the mechanistic aspects.

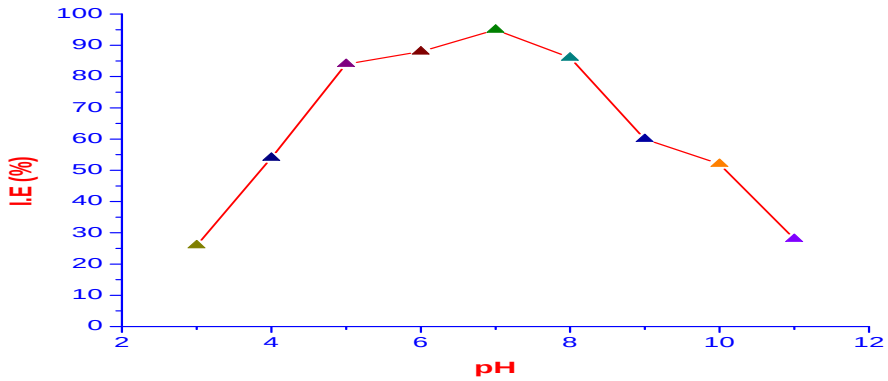

Figure 4: Effect of pH

3.2. Electrochemical impedance spectroscopy (EIS) measurements

EIS measurements were carried out to determine kinetic parameters for electron transfer reactions at the iron/electrolyte interface [23]. The corrosion behaviour of mild steel in aqueous solution containing 60 ppm Cl^- (control solution) with and without inhibitor was also investigated by EIS measurements.

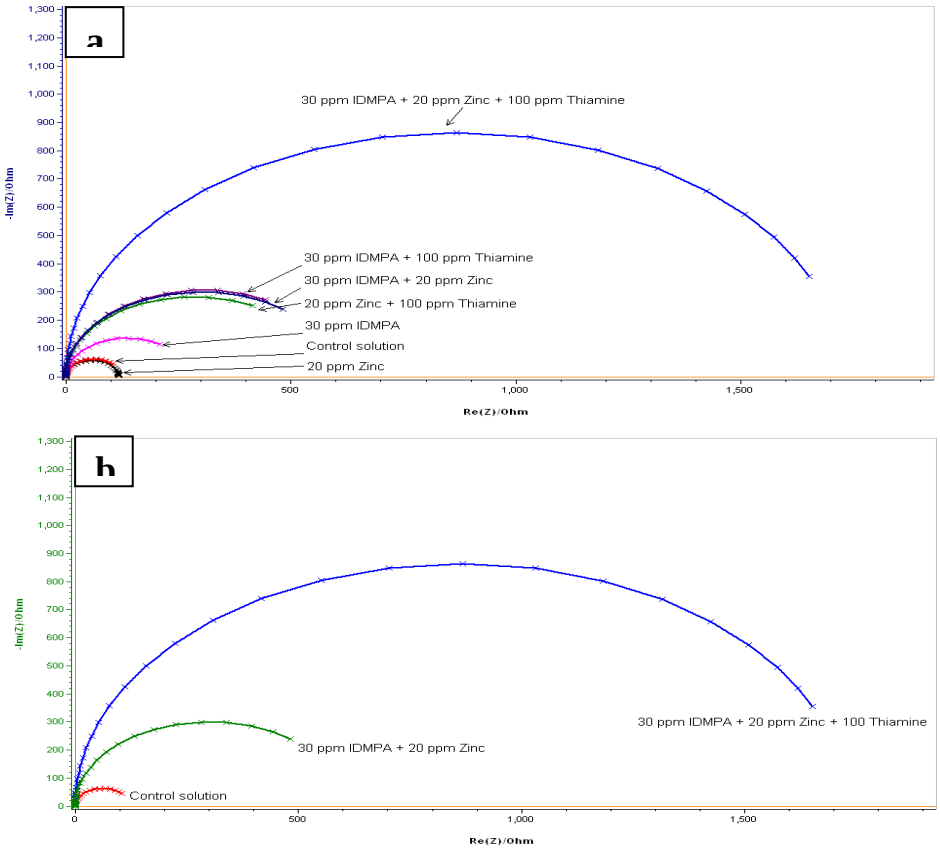

Figure 5: (a) Nyquist plots of mild steel immersed in various test solutions ; (b) Nyquist plots of mild steel immersed in control solution and inhibitor solution

The impedance parameters derived from these plots are given in the **Table 2**. **Fig. 5a** and **5b** show the impedance behaviour of mild steel corrosion in the form of Nyquist plots. From Nyquist plots in Fig. 5, it is clear that the impedance diagrams in most cases do not show a perfect semicircle. This behaviour can be attributed to the frequency dispersion as a result of inhomogenates of the electrode surface [24, 25]. These curves are dispersed in nature. Also these curves show a single semicircle indicating the occurrence of a single charge transfer reaction. All the Nyquist plots obtained in the present study are characterized by single time constant.

Table 2: A.C. impedance parameters of mild steel immersed in the presence and absence of inhibitor obtained by A.C. impedance spectra

Concentration (ppm)			Charge Transfer Resistance R_{ct} (Ω)	Double layer capacitance C_{dl} (μF/cm^2)	Constant exponent n	I.E (%)
IDMAP	Zn^{2+}	Thiamine				
0	0	0	125	20.34	0.59	-
30	0	0	273	4.25	0.88	54
0	20	0	117	22.97	0.96	-
30	20	0	597	0.89	0.70	79
30	0	100	605	0.85	0.78	79
0	20	100	568	0.99	0.78	78
30	20	100	1723	0.11	0.67	93

Fig. 6 shows the equivalent circuit based on the EIS data. Such an equivalent circuit was also discussed by several researchers [26-28] who obtained similar depressed semicircles with single time constant. In this equivalent circuit, R_s is the solution resistance between the reference and working electrode, R_{ct} is the charge transfer resistance corresponding to corrosion reaction at metal /electrolyte interface and CPE is the constant phase element. CPE is substituted for the respective capacitor of C_{dl} in order to fit the depressed semicircles better [29].
The impendence of CPE is defined as:

$$Z_{CPE} = Y_o^{-1}(j\omega)^{-n} \quad (6)$$

Where Y_o is the modulus, j is the imaginary root; $\boldsymbol{\omega}$ is the angular frequency and n is the surface irregularity [30]. Depending on the value of exponent n, Z_{CPE} represents a resistance with$R= Y^{-1}$; for n= -1, an inductance with C=Y [31]. The value range of a real electrode of n is often between 0 and 1. The smaller the value of n, the rougher the electrode surface and the more serious the corrosion of the electrode [32].
In the present study in the presence of the control alone, a small semicircle with an R_{ct} value of 125Ω and C_{dl} value of 20.34 µF/cm^{-1}is observed. A similar semicircle is also obtained when 20 ppm of Zn^{2+} is added to the control. Due to Zn^{2+}, R_{ct} is decreased to 117Ω and C_{dl} value is increased to 22.97µF/cm^{-1} in the value of n. These changes are due to the replacement of water molecules in the interface by zinc ions, which resulted in the increased rate of corrosion. By the addition of 30 ppm of IDMPA to the control, a single and slightly depressed semicircle with high R_{ct} value is obtained. The capacitance value is decreased and n value is increased. These observations can be attributed to the presence of organic inhibitor molecules in the double layer and the control of corrosion process to some extent.

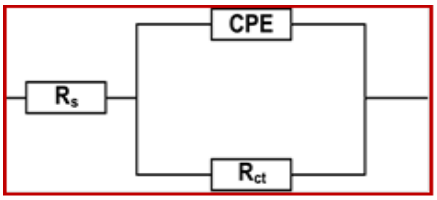

Figure 6: Nyquist plots are fitted by the equivalent electrical circuit

When the combination of 20 ppm Zn^{2+} and 30 ppm IDMPA, is considered in the presence of control, a large depressed semicircle is observed. The R_{ct} becomes dominant in the corrosion process due to the presence of a protective film on the metal surface. The R_{ct} value 597Ω is greater than that observed in case of the control. The C_{dl} is decreased to 0.89µF/cm^2 in the case of binary inhibitor formulations. IDMPA (30 ppm) + Zn^{2+} (20 ppm) + Thiamine (100ppm), the R_{ct} value is increased and the C_{dl} value is decreased. The value of R_{ct} in the case of the ternary formulation is increased manifold to 1723 Ω when compared to binary formulations. The C_{dl} value is found to decrease from 20.34µF/cm^2 for the control to 0.11µF/cm^2 in case of the ternary inhibitor formulations. This is because of the replacement of water molecules in the electrical double layer by the organic molecules having low dielectric constant [15]. The value of n is increased from 0.59 - 0.87 in the presence of the ternary inhibitor system, suggesting a decrease of inhomogenity of interface during inhibition. These results indicate that there is formation of non-porous and protective film in the presence of the ternary inhibitor formulation. The inhibition efficiency obtained from impedance studies is found to be 93%. Several authors who studied the inhibiting effects of phosphonate based corrosion inhibitors also reported that there is formation of thick and less permeable protective film on the metal surface [17, 33, 34]. They also conducted that the protective film consists of phosphonate-metal complexes. This result also implies the synergistic action operating between IDMPA, Zn^{2+} and Thiamine. This is in agreement with the inferences drawn from gravimetric studies

3.3. Potentiodynamic polarization studies
The potentiodynamic polarization curves of mild steel electrode in solution containing 60 ppm Cl^- at pH 7 in the absence and presence of various inhibitor combinations are shown in **Figs. 7a** and **7b**. The Tafel parameters derived from these curves and the inhibition efficiencies are listed in **Table 3**. For control solution, the values for the corrosion potential and corrosion current of -537 mV versus SCE and 22.87 µA/cm^2 are obtained. When IDMPA was alone added to control, the current potential is shifted to the negative side and its i_{corr} value is reduced to 14.57 µA/cm^2. The anodic Tafel (β_a) slope for IDMPA has been shifted more anodically (12 mV/decade) than the cathodic Tafel (β_c) slope (5 mV/decade). Similar observations were reported in the literature [17, 34]. In the case of addition of Zn^{2+} ions to the control, the corrosion potential is shifted to the

cathodic side and the shift in cathodic Tafel slope is greater and its i_{corr} value is reduced to 23.02 µA/cm^2. For a binary combination of 30 ppm IDMPA and 20 ppm Zn^{2+}, the corrosion potential is shifted to -557 mV versus SCE and its corrosion current density is also reduced to 13.76 µA/cm^2 when compared to the control.

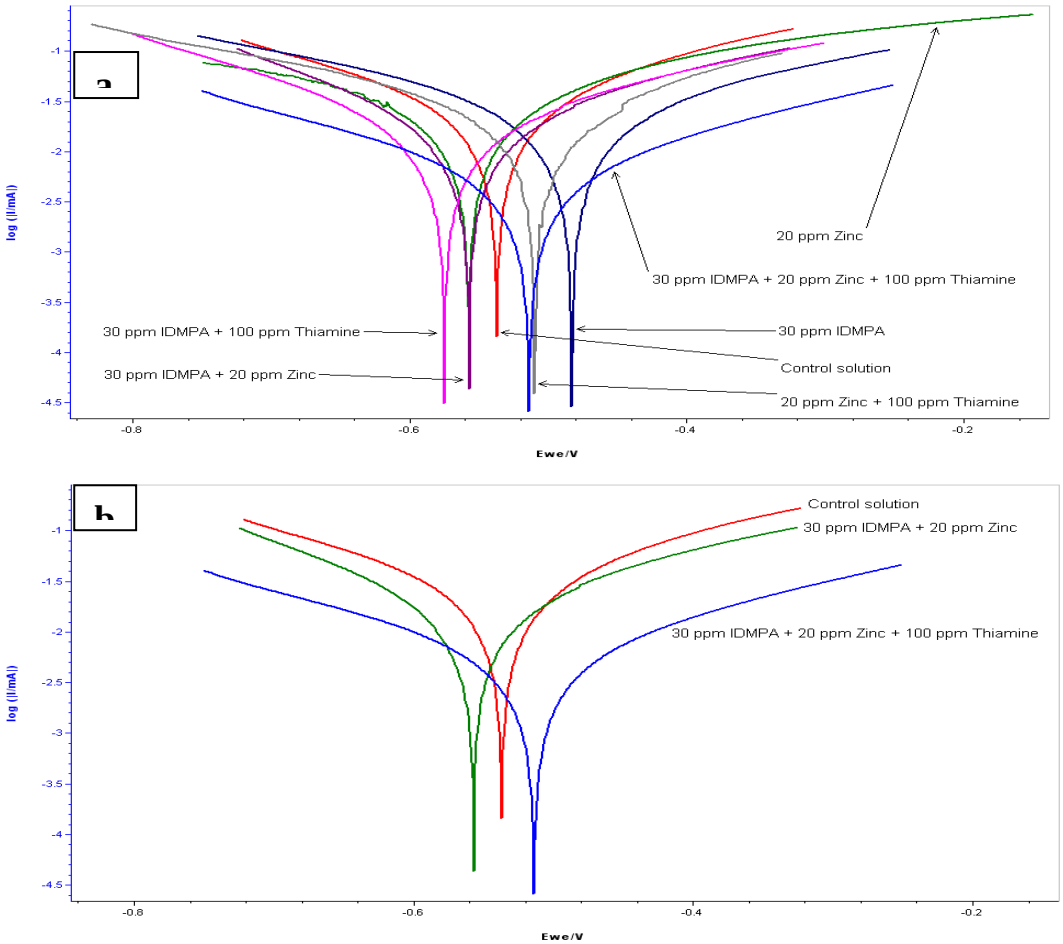

Figure 7: (a) Potentiodynamic polarization curves of mild steel immersed in various test solutions (b) Potentiodynamic polarization curves of mild steel immersed in control solution and inhibitor solution

Table 3: Corrosion parameters of mild steel immersed in the absence and presence of inhibitor obtained by potentiodynamic polarization studies

Concentration (ppm)			Tafel parameters				
IDMPA	Zn^{2+}	Thiamine	E_{corr} (mV vs SCE)	I_{corr} (µA/cm^2)	β_a (mV/decade)	β_c (mV/decade)	IE_p (%)
0	0	0	-537	22.87	191.09	179.44	-
30	-	-	-483	14.57	195.54	191.06	36
-	20	-	-557	23.02	228.99	193.50	-
30	20	-	-557	13.76	162.44	182.42	40
30	-	100	-575	13.03	170.68	181.88	24
-	20	100	-510	17.43	210.35	173.70	24
30	20	100	-514	3.72	190.02	186.99	84

The other two possible binary combinations viz., 30 ppm IDMPA with 100 ppm Thiamine and 20 ppm Zn^{2+} with 100 ppm Thiamine have also shifted corrosion potential to more cathodic side and decreased the corrosion current densities and its corresponding inhibition efficiencies each of 24 % is obtained. It is interesting to note that a mere addition of 100 ppm Thiamine to of 30 ppm IDMPA and 20 ppm Zn^{2+} has afforded the maximum inhibition efficiency of 84 %. The corrosion potential of the ternary combination is shifted to an extent of 23 mV versus SCE in the cathodic direction and its corresponding i_{corr} value is also largely reduced to 3.72 µA/cm^2. Moreover, in ternary combination, the shift in cathodic Tafel slope (8 mV/decade) is greater than

the shift in anodic Tafel slope shift (1 mV/decade). Since, both cathodic and anodic Tafel slopes have shifted, it can be interpreted that this ternary combination acts as a mixed inhibitor predominantly cathodic in nature. Similar phosphonate-based formulations were reported as mixed inhibitors in the literature [12, 17, 35]. A significant observation related to the inhibition efficiency values is to be noted. If the inhibition efficiency values obtained from gravimetric (IE_g), polarization (IE_p), and EIS (IE_i) studies are compared, differences are observed. It is suggested that the inhibition efficiency values obtained from various methods may not be strictly comparable when the immersion times used in these methods are not the same [15].

3.4. Fourier transform infrared spectroscopy

The FTIR spectrum of KBr pellet of pure IDMPA is shown in **Fig. 8a**. The characteristic band of phosphonic acid are due to the associate P=O stretching vibration 1140-1380 cm^{-1} and another band symmetric/asymmetric P-OH stretching vibrations at 1188–970 cm^{-1}[36]. The absorption peaks at 1020 cm^{-1}– 580 cm^{-1}, indicate the corrosion products of ferric hydroxide (γ–FeOOH) and magnetite (Fe_3O_4) respectively [37].

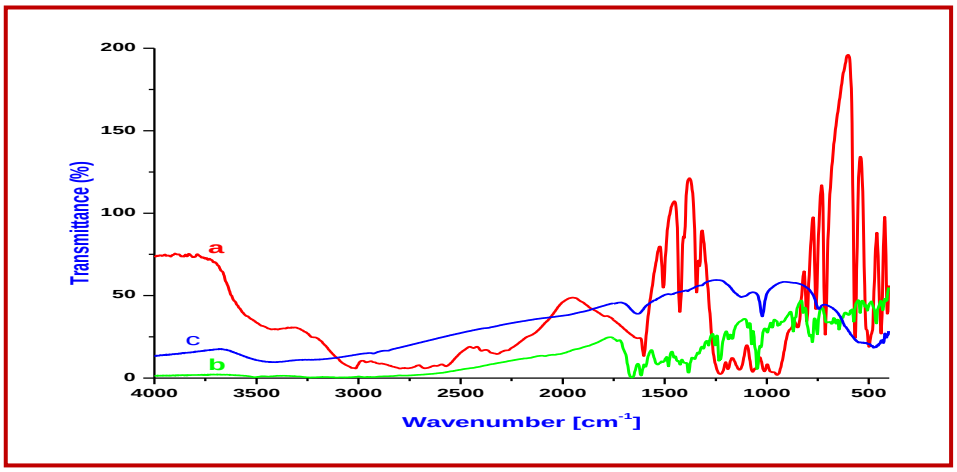

Figure 8: FTIR Spectra of (a) pure IDMPA (b) pure thiamine (c) surface film

The Pure IDMPA shows P=O stretching vibration at 1228.4 cm^{-1} and P-OH stretching vibration at 950 cm^{-1} .The broad absorption peak at 1602 cm^{-1} shows N-H stretching vibration. Carter et al [38] found that FT-IR spectra obtained with an organic phosphonate on a steel substrate are consistent with the phosphonate reaction on steel to produce metal salt. This shows that the phosphonates are coordinated with metal to form a metal phosphonate complex.

FTIR spectrum of pure Thiamine is shown in **Fig. 8b**. The pure Thiamine hydrochloride shows C=N stretching vibration at 1479 $cm^{-1}$and N-H stretching in the range 3436 cm^{-1}. The FTIR spectrum of protective film is shown in the **Fig. 8c**. The P=O stretching vibration shifts from 1228.4 cm^{-1} to 1124 cm^{-1}, the P-OH stretching has disappeared. The peaks observed around 1384 cm^{-1} indicate the presence of zinc hydroxide in the surface film [33, 39]. The N-Hstretching shows shift from 3436 to 3421 cm^{-1}. The C=N stretching shifts from 1479 cm^{-1} to 1461 cm^{-1}. These shifts would have been caused by the decrease in electron density of C-N bond and P-O bond due to shift of electron cloud density from N and O to Fe^{2+}. The IR results indicate the formation of a protective film contains [Fe(II)/Fe(III)-IDMPA-Thiamine], [Zn(II)-IDMPA–Thiamine], $Zn(OH)_2$ and small amount of oxides/hydroxide of iron.

3.5. Scanning electron microscopy

SEM analysis was carried out for characterizing the inhibitive film formed on the mild steel surface. **Fig. 9** shows the high resolution SEM images of the surfaces of mild steel immersed for seven days in the control in the absence and presence of the inhibitor, 30 ppm IDMPA, 20 ppm Zn^{2+} ions and 100 ppm Thiamine. **Figs. 9A** and **9B** reveals that the SEM pattern of specimen immersed in the absence of the inhibitor exhibits corrosion and also presence of different forms of iron oxides. The entire surface is covered by a scale-like black corrosion product, on which there is growth of another corrosion product appearing in the form of white clusters at several sites. **Figs. 9C** and **9D** show the morphological features of the inhibited surface. The corrosion product deposits observed in the case of the control are not present on the inhibited surface.It can be seen that the surface of the mild steel immersed in the inhibitors showed a smooth surface and there are no sites like pits and cracks indicating that the aggressive Cl^- ions have not penetrated because of the good surface coverage by the

inhibitive film. But a closer look at such sites reveals that the inhomogeneities are due to the structural defects of the metal substrate and that these sites are also covered by the inhibitor film.Thus, the inhibitor film covers the entire metal surface. This observation also accounts for the high inhibition efficiency values obtained during the gravimetric studies of the inhibitor system. From the SEM analysis it can be inferred that the inhibitor film exhibits good protective properties for mild steel in aqueous solution. So, SEM analysis shows the protective nature of the surface film [40].

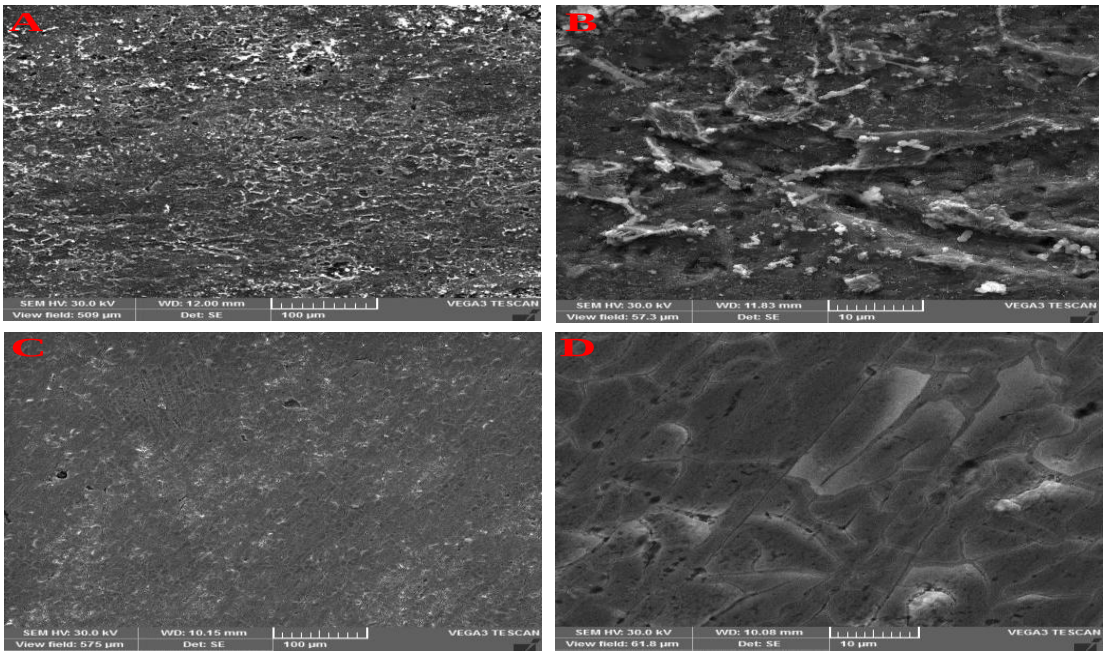

Figure 9: SEM images of mild steel immersed in A and B control solution, C and D inhibitor solution

3.6. Atomic force micrographs

Table 4 shows various AFM parameters obtained for the mild steel surface immersed in different environments. **Fig. 10** shows one &3-D images of polished metal surface immersed in 60 ppm Cl^- ion solution indicating the formation of iron oxides by the increased Rms value 95 nm and ΔZ value of 579.2 nm. **Fig. 11** shows one and 3-D images of mild steel immersed in 60 ppm Cl^- + 30 ppm IDMPA+ 200 ppm Zn^{2+} + 100 ppm Thiamine solution in which increased Rms value 57 nm and ΔZ value 91.58 representing the formation of protective thin film on the metal surface. These increased values strongly imply the formation of an inhibitive film by the addition of Zn^{2+} along with the phosphonic acid inhibitor system on the metal surface. These results are confirmed by the formation of protective layer by the inhibitor molecules [41-42].

Table 4: AFM parameters in different environments

Environment	Period of immersion	AFM Parameters	
		Rms value (nm)	ΔZ value (nm)
Polished metal + 60 ppm Cl^-	7 days	95	579.2
Polished metal + 60 ppm Cl^- + 30 ppm IDMPA + 20 ppm Zn^{2+} + 100 ppm Thiamine	7 days	57	91.58

3.7. Mechanism of protection

In order to explain all the experimental results, the following mechanism of corrosion inhibition can be proposed: When mild steel is immersed in neutral aqueous environment the anodic reaction is

$$Fe \rightarrow Fe^{2+} + 2e^- \quad (7)$$

Fe^{2+} further undergoes oxidation in the presence of oxygen available in the aqueous solution

$$Fe^{2+} \xrightarrow{[O_2]} Fe^{3+} + e^- \quad (8)$$

and the cathodic reaction is:

$$O_2 + 2H_2O + 4e^- \rightarrow 4OH^- \quad (9)$$

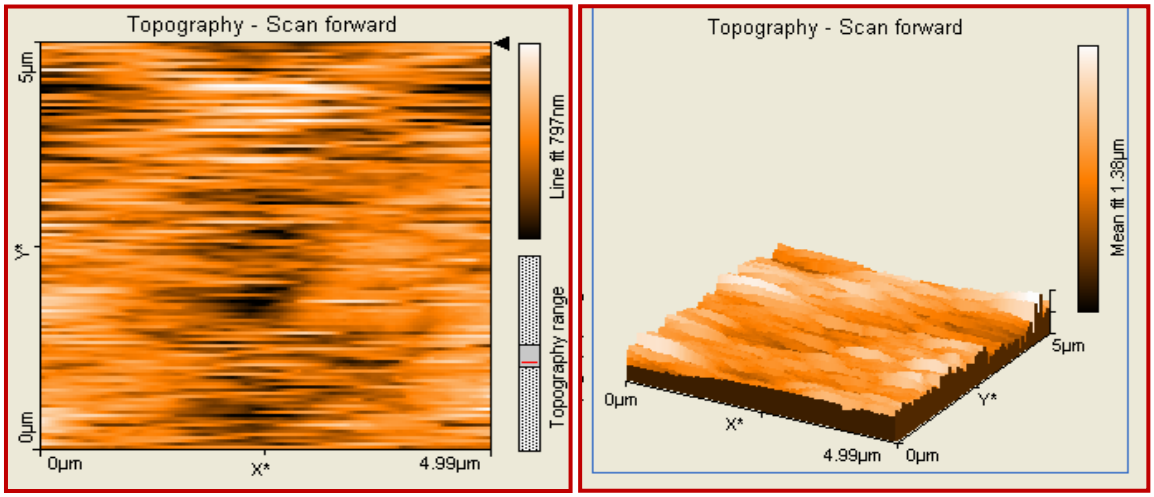

Figure 10: AFM images one 3D image of polished metal surface immersed in control solution

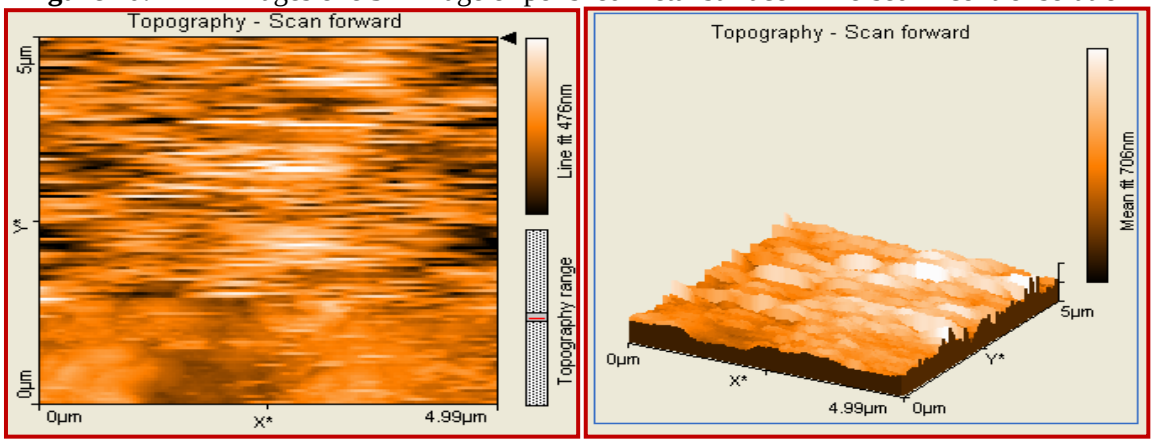

Figure 11: AFM images one and 3 D image of polished metal surface immersed in 60 ppm Cl- ion + 30 ppm IDMPA + 20 ppm Zn2+ + 100 ppm Thiamine

When the environment containing control solution (60 ppm Cl^- ions)/20ppm Zn^{2+}/30 ppm IDMPA/100 ppm Thiamine was prepared, a [Zn^{2+}-IDMPA-Thiamine] complex was formed in the solution. Besides this complex, there is presence of free IDMPA, Thiamine and Zn^{2+} ions. When the metal was immersed in this environment, the [Zn^{2+}-IDMPA-Thiamine] complex diffused from the bulk of the solution onto the surface of the metal and further complexes with Fe^{2+}/Fe^{3+} ions available due to initial corrosion. Free IDMPA and Thiamine molecules diffuse from bulk of the solution to the metal surface and form [Fe^{2+}/Fe^{3+}-IDMPA-Thiamine] complexes. These complexes fill the pores of the film formed on the surface and make it protective.

Free Zn^{2+} ions diffuse from the bulk of the solution to the metal surface and form $Zn(OH)_2$ at the local cathodic sites.

Thus, the corrosion is controlled by the protective film consisting of $Zn(OH)_2$ and metal-inhibitor complex, viz., [Fe^{2+}/Fe^{3+}-IDMPA-Thiamine]. Formation of $Zn(OH)_2$ controls the cathodic reaction and formation of (metal- inhibitor) complexes controls the anodic reaction. Hence, the inhibition is under mixed control. Similar reports of complex formation have been observed in the literature [12, 21, 41]. The mechanism has been justified by a scheme and a related model of the complex formed in the literature [20].

Conclusion

All the results showed that the IDMPA has excellent inhibition properties for the corrosion of mild steel in aqueous medium. The gravimetric measurements showed that the formulation containing 20 ppm Zn^{2+} ions and 30 ppm IDMPA and 100 ppm Thiamine yield good inhibition efficiency of 95%. Potentiodynamic polarization measurements showed that the IDMPA and Thiamine act as a mixed-type inhibitor both as anodic and cathodic. EIS measurements also indicate that the inhibiton increases, with increase the charge transfer resistance and showed that the inhibitive property depends on adsorption of the molecules on the metal surface. The new ternary inhibitor formulation Zn^{2+}-IDMPA-Thiamine shows excellent synergistic effect in corrosion control of mild steel. The inhibitor formulations Zn^{2+}-IDMPA-Thiamine are more effective in neutral aqueous medium (pH-7). In ternary formulation from gravimetric measurements, it is understood that the amount zinc released to the environment is less than 20 mg, thus it serves as an eco-friendly inhibitor. The results obtained from EIS, Potentiodynamic polarization and gravimetric studies are in good agreement. It's concluded that the above formulations can be used in cooling water systems.

Acknowledgements-One of the authors M. Prabakaran is grateful to the UGC for the fellowship under Research Fellowship in Sciences for Meritorious Students. Authors thank the Co-ordinator, UGC-SAP, Gandhigram Rural Institute for his help and also thank the authorities of Gandhigram Rural Institute for the encouragement.

References

1. Ali S. A., Saeed M. T., Rahman S.U., *Corros. Sci*. 45 (2003) 253.
2. Khaled K. F., Hackerman N., *Electrochim. Acta*. 48 (2003) 2715.
3. Fouda A.S., Ellithy A.S., *Corros. Sci*. 51 (2009) 868.
4. El-Taib Heakal F., Fouda A.S., Radwan M.S., *Mater. Chem. Phys*. 125 (2011) 26.
5. Fouda A.S., Abdallah M., Ahmed I.S., Eissa M., *Arabian. J. Chem*. 5 (2012) 297.
6. Chetouani A., Aouniti A., Hammouti B., Benchat N., Benhadda T., Kertit S., *Corros. Sci*. 45 (2003) 1675.
7. Bouklah M., Hammouti B., Lagrenée M., Bentiss F., *Corros. Sci*. 48 (2006) 2831.
8. Abdallah M., Helal E.A., Fouda A.S., *Corros. Sci*. 48 (2006) 1639.
9. Chetouani A., Hammouti B., Aouniti A., Benchat N., Benhadda T., *Prog.Org. Coat*. 45 (2002) 373.
10. Laamari M.R., benzakour J., Berrekhis F., Bakasse M., Villemin D., *J. Mater. Environ. Sci*. 3 (2012) 485.
11. Labjar N., EI Hajjaji S., Lebrini M., Serghini Idrissi M., Jama C., Bentiss F., *J. Mater. Environ. Sci*. 2 (2011) 309.
12. Amar H., Benzakour J., Derja A., Villemin D., Moreau B., Braisaz T., Tounsi A., *Corros. Sci*. 50 (2008) 124.
13. Rajendran S., Apparo B.V., Palaniswamy N., *Electrochim. Acta*. 44 (1998) 533.
14. Poczik P., Feliiosi I., Telgadi J., Kalaji M., Kalman E., *J. Serb. Chem. Soc*. 66 (2001) 859.
15. Apparao B.V., Christina K., *Indian J. Chem. Technol*. 13 (2006) 275.
16. Gunasekaran G., Natarajan R., Appa Rao B.V., Palaniswamy N., Muralidharan V.S., *Ind. J. Chem.Technol*. 5 (1998) 91.
17. Prabakaran M., Ramesh S., Periasamy V., *Res. Chem. Intermed.* 39 (2013) 3507.
18. Reznik L.Y., Sathler L., Cardoso M.J.B., Albuquerque M.G., *Mater. Corros*. 59 (2008) 685.
19. Gonzalez Y., Lafont M.C., Pebere N., Moran F., *J. Appl. Electrochem*. 26 (1996) 1259.
20. Sekine I., Hirakawa Y., *Corrosion*, 42 (1986) 272.
21. Apparao B.V., Srinivasarao S., *Mater. Corros.* 61 (2010) 285.
22. Sastri V.S., *Corrosion Inhibitors: Principles and Applications*, John Wiley and Sons, New York, (1998).
23. Sayed El., Sherit M., *Mater. Chem. Phys*. 129 (2011) 961.
24. Juttner K., *Elecrochim. Acta*. 35 (1990) 1501.
25. Benali O., Benmehdi H., Hasnaoui O., Selles C., Salghi R., *J. Mater. Environ. Sci*. 4 (2013) 127.
26. Alagta A., Felhosi I., Telegdi J., Bertoti I., Kalman E., *Corros. Sci*. 49 (2007) 2754.
27. Gunasekaran G., Chauhan L.R., *Electrochim. Acta*. 49 (2004) 4387.
28. Ebenso E.E., Kabanda M.M., Murulana L.C., Singh A.K., Shukla S.K., *Ind. Eng. Chem. Res*. 51 (2012) 12940–12958.
29. Macdonald J.R., Johnson W.B., *Impedance Spectroscopy*, John Wiley and Sons, New York, (1987).
30. Li G.Y., Ma H.Y., Jiao Y.L., Chen S.H., *J. Serb. Chem Soc*. 69 (2004) 791.
31. Macdonald J.R., *J. Electroanal. Chem*. 223 (1987) 25.
32. Khaled K.F., Hackerman N., *Electrochim. Acta*. 49 (2004) 485.
33. Felhosi I., Keresztes Z.S., Karman F.H., Mohai M., Bertoti I., Kalman E., *J. Electrochem. Soc*. 146 (1999) 961.
34. Pech Canul M.A., Chi Canul L. P., *Corrosion*. 55 (1999) 948.
35. To X. H., Pebere N., Pelaprat N., Boutevin B., Hervaud Y., *Corros. Sci*. 39 (1997) 1925.
36. Colthup N.B., Daly L.H., Wiberley S.E., *Introduction to Infrared and Raman Spectroscopy*, 3rd ed, Academic press, New York, (1990).
37. Nakamoto K., *Infrared and Raman Spectra of Inorganic and Coordination Compounds*, 4th ed, John Wiley and Sons, New York, (1986).
38. Carter R.O., Gierczak C.A., Dickie R.A., *Appl. Spectros*. 40 (1986) 649.
39. Wang C.T., Chen S.H., Ma H.Y., Wang N.X., *J. Serb. Chem. Soc*. 67 (2002) 685.
40. Yadav D. K., Quraishi M.A., *Ind. Eng. Chem. Res*. 51 (2012) 14966.
41. Prabakaran M., Venkatesh M., Ramesh S., Periasamy V., *Appl. Surf. Sci.* 276 (2013) 592.
42. Khaled K. F., *Int. J. Electrochem. Sci.* 8 (2013) 3974.